



Review

A state-of-the-art review of parameters influencing measurement and modeling of skid resistance of asphalt pavements



Reginald B. Kogbara ^{a,*}, Eyad A. Masad ^{a,b}, Emad Kassem ^c, A. (Tom) Scarpas ^d, Kumar Anupam ^d

^a Mechanical Engineering Program, Texas A&M University at Qatar, P.O. Box 23874, Education City, Doha, Qatar

^b Zachry Department of Civil Engineering, Texas A&M University, College Station, TX 77843, USA

^c Department of Civil Engineering, University of Idaho, Moscow, ID 83844, USA

^d Section of Pavement Engineering, Faculty of Civil Engineering and Geosciences, Delft University of Technology, Stevinweg 1, Delft, The Netherlands

HIGHLIGHTS

- A state-of-the-art review of skid resistance of asphalt pavements is presented.
- Key parameters influencing skid resistance measurement and modeling are discussed.
- Details modeling efforts entailing different aspects of tire-pavement interaction.
- Frictional performance of asphalt pavements largely depends on coarse aggregates.
- Some research gaps and ongoing efforts to address some of the gaps are identified.

ARTICLE INFO

Article history:

Received 11 February 2016

Received in revised form 29 March 2016

Accepted 1 April 2016

Available online 6 April 2016

Keywords:

Aggregate properties

Asphalt mixtures

Skid resistance

Surface texture

Friction

ABSTRACT

A state-of-the-art review of key parameters that influence measurement and modeling of skid resistance of asphalt pavements is provided. Tire-pavement interaction/friction is discussed and the current harmonization method of friction measurements questioned. The latest developments on pavement surface texture measurement and characterization are highlighted. A critical review of aggregate properties affecting friction, the frictional properties of asphalt mixtures and the influence of environmental factors on skid resistance is presented. An overview of modeling efforts entailing different aspects of tire-pavement friction is also presented. The frictional performance of asphalt pavements largely depends on the type and quality of coarse aggregates used. The different hot mix asphalt (HMA) classifications generally have similar microtextures. Their frictional performance follows the same order as their macrotextures. There is need for experimentally-validated skid resistance prediction models, especially for warm surfaces. Such models should account for tire and pavement surface texture characteristics, and the influence of environmental factors. Some other research needs are also identified.

© 2016 Elsevier Ltd. All rights reserved.

Contents

1. Introduction	603
2. Tire-pavement interaction/friction	603
2.1. Mechanisms of pavement friction	604
2.2. Measurement of pavement friction	604
2.3. Harmonization of pavement friction measurements	604
3. Pavement surface texture	607
3.1. Pavement texture measurement	607
3.2. Pavement texture characterization	608
4. Aggregates and asphalt mixture characteristics	609
4.1. Aggregates properties affecting friction	609

* Corresponding author.

E-mail address: regkogbara@cantab.net (R.B. Kogbara).

4.1.1.	Hardness and mineralogy	609
4.1.2.	Polish resistance	609
4.1.3.	Abrasion/wear resistance	609
4.1.4.	Shape, texture and angularity	609
4.1.5.	Soundness	609
4.1.6.	General comments	609
4.2.	Frictional properties of asphalt mixtures	610
5.	Influence of environmental factors on skid resistance	611
5.1.	Influence of temperature	611
5.2.	Influence of rainfall	612
5.3.	Influence of contaminants	612
6.	Modeling of tire-pavement friction	612
6.1.	Pavement surface texture and roughness modeling	612
6.2.	Tire rubber modeling	612
6.3.	Tire-pavement contact modeling	613
6.4.	Modeling of asphalt mixtures	613
6.5.	Pavement surface skid resistance modeling	614
7.	Concluding remarks	614
	Acknowledgements	615
	References	615

1. Introduction

Skid resistance is defined as the force developed when a tire that is prevented from rotating slides along the pavement surface [1]. It is a property of the road surface which characterizes road pavement roughness and impact on friction forces when the pavement is exposed to the wheel load [2]. The skid resistance of an asphalt pavement is an important parameter that influences driving safety on a road. Especially, as it has been shown that there is a linear relationship between slipperiness of the pavement surface and crashes [3]. Moreover, several studies show a dramatic increase in accident risk when the friction numbers decrease below certain threshold values [4].

Skid resistance/friction have two components, namely, adhesion and hysteresis [5]. These components largely depend on two properties of the pavement surface, vis-à-vis, macrotexture and microtexture. The aforementioned terms are discussed subsequently. The skid resistance of an asphalt pavement evolves over time and is affected by environmental factors. High ambient and pavement surface temperatures could significantly influence the reliability of skid resistance measurements [6]. Therefore, a fundamental understanding of the influence of the aforementioned parameters on skid resistance is crucial. Predictive models for skid resistance evolution are also necessary for design and construction of pavements with adequate friction.

Several studies have reviewed different aspects of, and some parameters influencing tire-pavement friction and skid resistance

[3,7–15]. However, very few have considered in depth the influence of several of the aforementioned parameters and skid resistance modeling efforts in a single work. Moreover, the subject matter is a fast evolving research area. Hence, there is need to keep researchers and practitioners abreast with the latest developments in the field. Thus, this paper seeks to provide a concise but critical review of the state-of-the-art on measurement and modeling of asphalt pavement skid resistance. It combines information on different parameters associated with skid resistance of asphalt pavements, which are ordinarily the subjects of entire reports. These include tire-pavement friction, and pavement surface texture measurement and characterization. Other areas reviewed are aggregate properties affecting friction, the frictional properties of asphalt mixtures and the influence of environmental factors on skid resistance. Modeling efforts on tire-pavement friction are also discussed.

2. Tire-pavement interaction/friction

The skid resistance of a pavement surface mainly refers to the contribution of the pavement surface to tire-pavement interaction and the resulting friction force [9]. Changes in speed or direction of a vehicle, the resulting acceleration, braking or turning leads to development of forces at the tire-pavement interface. Such forces cause a reaction (called friction) between the tire and pavement that facilitates the afore-mentioned vehicular movements. Thus, tire-pavement friction is critical to reduction of potential road crashes. It has been historically emphasized that most skidding problems occur due to friction deficiencies from wet pavements [11]. Nevertheless, a recent study showed that friction impacts the rate of dry condition crashes as well [16]. Hence, more crashes occurs on roads with low friction than on those with high friction [3].

Pavement friction has been defined as “the force that resists the relative motion between a vehicle tire and a pavement surface” [7]. A dimensionless coefficient, known as the coefficient of friction (μ) is usually employed for characterizing tire-pavement friction. The friction coefficient between a tire and a pavement surface can be defined as the quotient of the tangential force at the tire-pavement contact interface and the longitudinal force on the wheel. Fig. 1 illustrates the above definition (braking wheel).

From Fig. 1, the friction coefficient (μ) is given as:

$$\mu = \frac{F}{F_w} \quad (1)$$

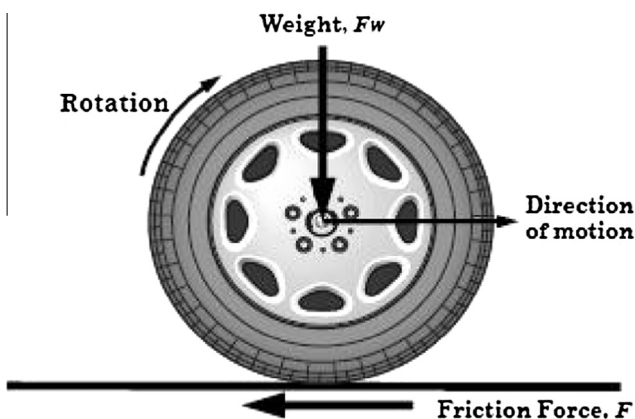


Fig. 1. Illustration of forces acting on a rotating tire (after Hall et al., 2009).

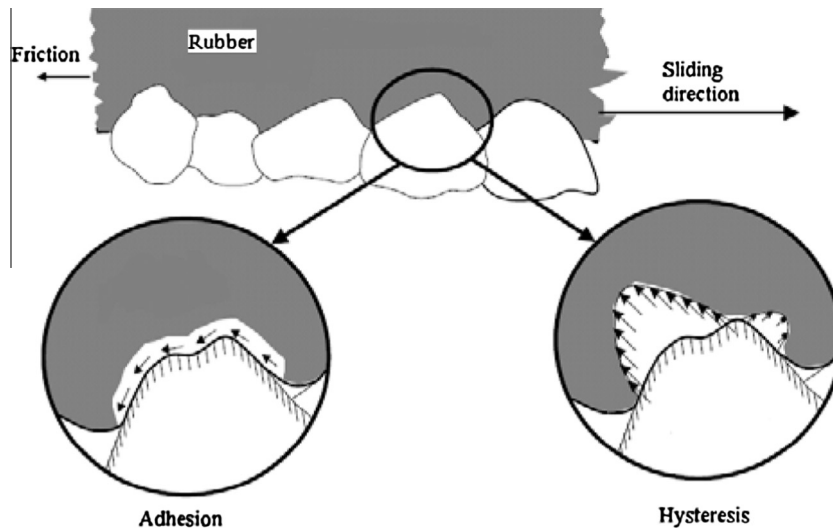


Fig. 2. Key mechanisms of tire-pavement friction (after Hall et al., 2009).

Tire-pavement friction is affected by several factors. These include pavement surface characteristics, tire properties, vehicle operating parameters and environmental factors. The microtexture, macrotexture, pavement materials properties and slip speed are the factors that can easily be controlled through pavement design and speed limit regulations. Details of these factors can be found elsewhere [3].

2.1. Mechanisms of pavement friction

Pavement friction is occasioned by the combination of two mechanisms, namely, adhesion and hysteresis (Fig. 2). Adhesion emanates from molecular bonds in areas of high local pressure resulting from unevenness in the road surface. Hysteresis is due to energy loss resulting from the deformation of the tire rubber around the protuberances and depressions in the pavement surface [5]. In addition to the aforementioned mechanisms, there are also two other components of rubber friction with little significance. These are frictional contributions from rubber wear, and surface (or micro) hysteresis as opposed to bulk hysteresis. The cohesion loss component of friction from rubber wear was verified through testing within the last decade [17,18].

2.2. Measurement of pavement friction

The measurement of pavement friction is not an easy task as the frictional forces being measured are sensitive to a number of factors difficult to control. Such factors include those from the pavement – namely, texture, temperature, chemistry of materials, etc. Others are from the tire (tread design, rubber composition, sliding velocity temperature, etc) and fluid/contaminant (viscosity, density, film thickness, etc). However, during friction measurement, all other factors except the road surface are kept constant. The pavement surface is then wetted with a specified amount of water and a standardized measuring tire used on friction measuring equipment to measure the pavement friction.

There are several equipment for friction measurement. Table 1 summarizes a range of some commonly used friction measuring devices. The three major operating principles of frictional measuring equipment are, longitudinal friction coefficient (LFC), sideways force coefficient (SFC) and sliders or stationary or slow-moving measurement principles. The LFC principle entails the creation of controlled sliding process of the tire through the application of a

braking force. This blocks the vehicle wheel such that it rotates more slowly than the forward speed of the vehicle. Devices operating on this principle employ a wide range of slip ratios, which is used to assess and compare tire and vehicle speeds [2,11]. The slip ratio is expressed mathematically as follows [3]:

$$SR = \frac{V - V_p}{V} \times 100 = \frac{S}{V} \times 100 \quad (2)$$

where SR is slip ratio, V is vehicle directional speed (mph), V_p is average peripheral speed of tire (mph) and S is the slip speed (mph). The absolute value of SR is normally used, otherwise there will be negative values for acceleration when $V_p > V$.

The SFC principle uses an instrumented measuring wheel set at an angle (called slip angle) to the direction of travel of the vehicle [11]. The slip angle induces friction between the tire and road as it makes the tire slip over the road surface. The resulting force (sideways force) along the wheel axle is then measured [2,11]. The SFC is then expressed as the ratio of the sideways force to the vertical reaction between the tire and the pavement surface. Sliders or stationary or slow-moving measurement principle covers devices mostly used for stationary testing. Laboratory devices mostly fall under this group. These devices use rubber sliders that are attached either to the foot of a pendulum arm or to a rotating head, which slow down on contact with the pavement surface. Continuous Friction Measuring Equipment (CFME) provide greater detail about spatial variability of tire-pavement frictional properties. They operate on LFC or SFC principles, and have gained increased attention around the world [11]. Details of commonly used CFMEs are available from Yager [21]. CFME measurements are reported to be sensitive to water film thickness and testing speed. Measurements by the GripTester – a CFME are also reported to be affected by grade suggesting greater accuracy mainly on flat surfaces [22].

2.3. Harmonization of pavement friction measurements







Different friction measuring equipment gives different values for the same pavement surface. Hence, harmonization is used to adjust the outputs of the different equipment so that they all report the same value for the same pavement condition. The Permanent International Association of Road Congress (PIARC) developed the international friction index (IFI) to compare and harmonize different friction measurement methods [23]. The IFI consists of a speed constant and a friction number at 60 km/h.

Table 1
Summary of friction/skid resistance measuring devices [2,19,20].

Title	Measurement principle	Main parameters	Tire and wheel load	Measurement device view
ADHERA	Longitudinal friction coefficient (LFC)	Water film thickness: 1.0 mm; Measures macrotexture; Measurement speed: 40, 60, 90, 120 km/h; Measurement interval: 20 m	PIARC smooth profile tire 165R15 (180 kPa); Wheel load: 2500 N	
BV-11	Longitudinal friction coefficient (LFC)	Slip ratio: 0.17 or 17%; Water film thickness: 0.5–1.0 mm; Measurement speed: 70 km/h; Measurement interval: 20 m	Trelleborg type T49 tire (140 kPa); Wheel load: 1000 N	
GripTester	Longitudinal friction coefficient (LFC)	Slip ratio: 0.15 or 15%; Water film thickness: 0.5 mm; Measurement speed: 5–100 km/h; Measurement interval: 10–20 m or other	254 mm diameter smooth profile ASTM-tire (140kPa); Wheel load: 250 N	
RoadSTAR	Longitudinal friction coefficient (LFC)	Slip ratio: 0.18 or 18%; Water film thickness: 0.5 mm; Measures macrotexture; Measurement speed: 30, 60 km/h Measurement interval: 50 m	PIARC tire with tread; Wheel load: 3500 N	
ROAR DK	Longitudinal friction coefficient (LFC)	Slip ratio: 0.2 or 20%; Water film thickness: 0.5 mm; Measures macrotexture; Measurement speed: 60, 80 km/h Measurement interval: >5 m	ASTM 1551 tire (207 kPa); Wheel load: 1200 N	
ROAR NL	Longitudinal friction coefficient (LFC)	Slip ratio: 0.86 or 86%; Water film thickness: 0.5 mm; Measures macrotexture; Measurement speed: 50, 70 km/h Measurement interval: 5–100 m	ASTM 1551 tire (200 kPa); Wheel load: 1200 N	
RWS NL Skid Resistance Trailer	Longitudinal friction coefficient (LFC)	Slip ratio: 0.86 or 86%; Water film thickness: 0.5 mm; Measurement speed: 50, 70 km/h; Measurement interval: 5–100 m	PIARC smooth profile tire 165R15 (200 kPa); Wheel load: 1962 N	
SCRIM	Sideway friction coefficient (SFC)	Slip angle: 20°; Water film thickness: 0.5 mm; Measures macrotexture; Measurement speed: 50 km/h; Measurement interval: >10 m	Avon SCRIM smooth profile tire 76/ 508 (350 kPa); Wheel load: 1960 N	
Skiddo-meter BV-8	Longitudinal friction coefficient (LFC)	Slip ratio: 100% or 14%; Water film thickness: 0.5 mm; Measurement speed: 40, 60, 80 km/h; Measurement interval: 30–50 m	AIPCR tire with longitudinal tread 165R15; Wheel load: 3500 N	
SKM	Sideway friction coefficient (SFC)	Slip angle: 20°; Water film thickness: 0.5 mm; Measurement speed: 50 km/h; Measurement interval: 100 m or other	Smooth profile tire; Wheel load: 1960 N	
SRM	Longitudinal friction coefficient (LFC)	Slip ratio: 15% or 100%; Water film thickness: 0.5 mm; Measurement speed: 40, 60, 80 km/h; Measurement interval: 20 m or other	AIPCR tire with longitudinal tread 165R15; Wheel load: 3500 N	
TRT	Longitudinal friction coefficient (LFC)	Slip ratio: 25%; Water film thickness: 0.5 mm; Measurement speed: 40–140 km/h; Measurement interval: 20 m or other	Smooth profile ASTM tire; Wheel load: 1000 N	

(continued on next page)

Table 1 (continued)

Title	Measurement principle	Main parameters	Tire and wheel load	Measurement device view
SRT-3	Longitudinal friction coefficient (LFC)	Slip ratio: 100%; Water film thickness: 0.5 mm; Measurement speed: 60 km/h	Tire with tread (200 kPa)	
IMAG	Longitudinal friction coefficient (LFC)	Slip ratio: 100%; Water film thickness: 1.0 mm; Measurement speed: 65 km/h	PIARC smooth profile tire; Wheel load: 1500 N	
DFT Dynamic Friction Tester	Rotating friction	For stationary measurements	-	
SRT Pendulum	Pendulum test	For stationary measurements	-	
T2GO	Slow-moving measurement; Longitudinal friction coefficient (LFC)	Slip ratio: 20%; Used for pedestrian/bicycle paths, road marking	Two 75 mm width tires	
VTI Portable Friction Tester (PFT)	Slow-moving measurement; Longitudinal friction coefficient (LFC)	Used for pedestrian/bicycle paths	-	

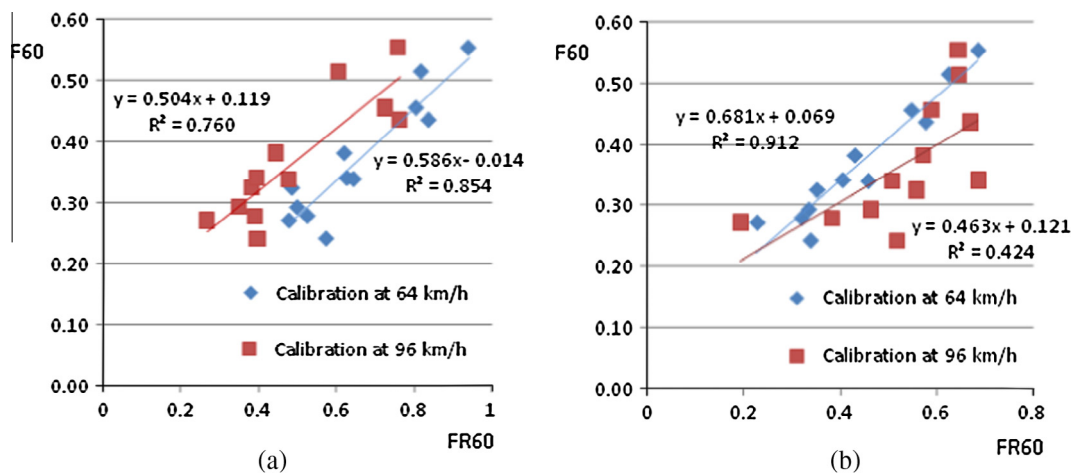


Fig. 3. Quality of IFI calibration for two different friction measuring equipment (a) run way friction tester, and (b) locked wheel skid tester at two different speeds [25]. Note: F60 is the same as FI and FR60 is the same as F in Eq. (3).

The speed constant is determined by a macrotexture measurement. A macrotexture measurement is required because the influence of the slip speed on the friction value varies with different pavement macrotextures [4]. Hence, given a friction measurement at a certain slip speed coupled with a macrotexture measurement,

the friction at any slip speed for that device can be deduced. This method is also covered by the ASTM E1960 standard [24]. The friction index equation is given by [23]:

$$FI = A + B \times F \times e^{\frac{S-60}{Sp}} + C \times Tx \tag{3}$$

where FI is the friction index at 60 km/h slip speed; A, B and C are device specific constants or calibration factors for the friction equipment used: for smooth tires, the constant C = 0. F and S are the measured friction, and slip speed at which the friction was measured, respectively. S_p is the speed constant or golden value speed number. Tx is a measure of the macrotexture (for e.g. mean profile depth, MPD in mm).

The speed constant (S_p) in Eq. (3) can be obtained from the following equation:

$$S_p = a + bTx \quad (4)$$

where a and b are constants depending on the macrotexture measuring device and can be given values of 14.2 and 89.7 as per ASTM E1960 [24].

There are criticisms on the inconsistency of this harmonization method. For instance, the FI at 60 km/h slip speed from the same equipment estimated from friction measurements at two different speeds on the same pavement showed considerable variations. Moreover, the assumption of linearity between the FI at 60 km/h slip speed, and the measured friction (F) at a different slip speed adjusted to 60 km/h slip speed using Eq. (3), may not be valid in some situations. Fig. 3 illustrates the above. It questions the linearity between the FI and the F (Eq. (3)) especially at 96 km/h speed. Other deficiencies of the IFI method has also been identified. These include its failure to compensate for disparity in measurements due to differences in properties of the measuring mechanism such as different inflation pressures. The impractical requirement of an extra set of spot texture measurements on the pavement surface in busy areas was also highlighted. Consequently, the Lund-Grenoble (LuGre) model has been suggested as a superior alternative to the underlying model used in the ASTM E1960 standard. Friction measurements by different equipment have been accurately predicted via non-linear optimization of LuGre model parameters. These are documented elsewhere [25].

3. Pavement surface texture

Pavement surface texture is simply defined as the deviations of the pavement surface from a true planar surface [3]. The scales of surface texture have been defined by PIARC according to the wavelengths of the deviations [26]. Thus, pavement texture is divided into:

- Microtexture* with wavelengths from 0 mm to 0.5 mm.
- Macrotexture* with wavelengths from 0.5 mm to 50 mm.
- Megatexture* with wavelengths from 50 mm to 500 mm.
- Unevenness* with wavelengths from 500 mm to 50 m.

These texture scales have different contributions to tire-pavement friction. The microtexture is the surface roughness of a pavement at the microscopic level [27]. It can be described as the fine-scale texture on the surface of the coarse aggregate particles in asphalt, which interacts with the tire rubber on a molecular scale and provide adhesion. It is of fundamental importance on both wet and dry pavements and needs to be present at any speed [9,11]. Further, the microtexture of aggregates helps cut through the water film between the aggregate particle and the tire rubber, thus playing an important role in wet skid resistance [28].

The macrotexture is typically formed by the shape and size of the aggregate particles in the pavement surface or by grooves in some surface. It is also affected by the spacing and arrangement of coarse aggregate particles. It governs skid resistance on wet pavements, with skid resistance decreasing as speed increases. Surfaces with greater macrotexture generally have higher friction at high speeds than at low speeds [29] but this is not always the

case [11]. The macrotexture is responsible for a large portion of pavement friction at vehicle speeds above 90 km/h on wet pavements regardless of the slip speed [3]. It affects water drainage from the tire footprint and hence, it is thought to be responsible for friction due to hysteresis at high speeds [9]. The megatexture can be described by ruts, potholes, major joints and cracks. It affects vibrations in the tire walls and is therefore linked to noise and rolling resistance. Unevenness is usually caused by construction defects or deformation due to vehicular loading of the pavement. It affects vehicle dynamics, ride quality and pavement drainage and can also diminish tire-pavement contact [9]. Micro- and macrotexture are essential, while megatexture and unevenness are undesirable for optimum pavement performance [30].

Pavement texture is affected by a number of factors. These depend on the materials comprising a pavement, vis-à-vis, aggregate, binder and asphalt mix properties as well as post-placement treatment. The main factors that affect the macrotexture and microtexture are listed as follows. The macrotexture is affected by the maximum aggregate size, coarse and fine aggregate types, mix binder content and viscosity, mix gradation and mix air content. While the microtexture is mainly affected by the coarse aggregate type [3].




3.1. Pavement texture measurement

Majority of the generally used methods for pavement texture measurement are for the macrotexture. These are mostly rubber-on-road techniques. More recent developments revolving around non-contact measurements are geared towards microtexture measurements. The most common macrotexture measuring equipment are volumetric sand patch method, circular texture meter and the outflow meter. There are also laser-based (or electro-optic) methods for high speed friction measurements. The details of these equipment, and their advantages and disadvantages have been reviewed [3]. Table 2 shows the same information for more recent laser-based, stereo photogrammetry, and microscopy methods used for measurement of different texture scales.

The portable Model 9300 laser texture scanner (LTS) from Ames Engineering is a more recent laser-based equipment. It is capable of determining a range of texture parameters (see Table 2). These are applicable for estimation of the macrotexture and some of the microtexture within 0.03–0.5 mm wavelengths [31]. Albeit, microtexture determination may only have high accuracy within the wavelength range not shorter than the equipment's spot size of 0.05 mm. Studies have evaluated deployment of 3D modeling and areal texture parameters for a better understanding of pavement surface texture at its different wavelengths. Laser scanners such as the triangulation types, which allow the calculation of new texture indicators, have been used to produce 3D models. Such indicators, which refer to surfaces and volumes, permit a more stable and complete texture characterization [32]. However, laser scanners are quite expensive.

In light of the high cost of laser-based systems, more recent research have considered 3D measurements of surface texture using microscopy and stereo photogrammetry (Table 2). Measurements in 3D gives an indication of the extent of physical changes that cannot be achieved using 2D line profiles. Large amount of data can be collected, which could likely improve the statistical significance of surface roughness calculations. Qualitative observations of changes occurring on surfaces of aggregates during the polishing process have been successfully made using 3D focus variation microscopy. The corresponding roughness was then characterized using areal roughness parameters and data filtering techniques. Roughness parameters used include height (arithmetic mean height, skewness, kurtosis, etc) and volume (void volume

Table 2
Overview, advantages and disadvantages of pavement surface texture measurement methods [33,34].

Method/equipment	Description	Equipment photograph and details	Parameters measured	Advantages	Disadvantages
Laser method	Non-contact lasers or laser texture scanners (LTS) scan and precisely measure surface elevations at intervals <0.25 mm. More recent LTS capable of measuring texture profiles with wavelengths down to 0.05 mm	 <i>LTS from Ames Engineering</i>	Computes MPD, estimated texture depth (ETD), texture profile index (TPI), RMS, and band passed filtered elevation and slope variance	Results found to correlate well with the sand patch method [34]. It can also cover key wavelengths in the microtexture scale of texture. Laser method collects continuous data at high speeds	Laser systems are very expensive. Skilled operators are required for data collection and processing. As regards microtexture data, it omits wavelengths < laser spot size
Close range (stereo) photogrammetry and micro-scopy	Based on (stereo) images captured by camera or microscope and analyzed using proprietary software for 3D modeling of the captured surface	 **  ***	Provides threshold mean texture depth (TMTD) [*] . The software (s) output void and material volume, and surface height parameters	Inexpensive equipment, ability to visualize surface texture in 3D. Correlates well with MTD from sand patch test ($R^2 = 0.9$). Covers micro, macro and mega texture scales	Accuracy depends on user-adopted imaging set up, lens optics and eliminating the effect of camera shake. Requires skill and software for analysis of 3D models

CCD: Charge coupled device, DFT: Dynamic friction tester, LCD: Liquid-crystal display, MPD: Mean profile depth, MTD: Mean texture depth, RMS: Root mean squared. ^{*}TMTD: New 3D model measure of macrotexture, ^{**}Canon digital SLR camera, ^{***}Alicona infinite focus microscope.

and material volume) parameters. Some of these parameters correlated well with friction [9,35].

Stereo photogrammetry involves estimating 3D co-ordinates of points on an object using measurements from multiple images taken from different positions. Studies have investigated use of a version of stereo photogrammetry, close range photogrammetry (CRP), for texture measurements. The CRP technique entails use of an ordinary camera to capture multiple (stereo) images of the pavement surface. Three dimensional models of the surface texture are then produced and analyzed from the captured images using proprietary software including 3D flow Zephyr, Digital Surf MountainsMap, etc [33,36,37]. The CRP technique has been used for assessments of micro, macro and megatexture scales [28,38–40].

3.2. Pavement texture characterization

There are a number of standard parameters used for characterization of pavement surface macrotexture. The most common parameters used are the MTD, MPD and sensor measured texture depth (SMTD). The commonly used sand patch method gives the MTD as the ratio of volume to the total area covered. The latter term is deduced from the diameter of the area covered by the glass spheres (sand was formerly used) spread on the surface. A laser-based system can be used to generate a set of measurements thus creating a surface profile. Thereafter, an algorithm summarizes the data into a single average. This single average may be expressed as the MPD or the SMTD. The MPD is defined as the average of all the mean segment depths of all the segments of the profile [41]. It measures the height of the highest peaks above the mean level

[9]. While the SMTD is a root mean square (rms) measure of the texture above and below a mean level. Laser systems software also output characteristic parameters for the vertical, horizontal and synthesized extension of surface profile irregularities. Vertical extension parameters include the arithmetic mean and RMS deviation of the profile. While horizontal extension parameters include the average and RMS wavelength of the profile [42].

There are no standardized methods for microtexture characterization. Albeit, a test method, ASTM E303–93 [43], provides a measure of microtexture as a frictional property of surfaces using the British Pendulum Tester (BPT). It has been deployed for measuring the microtexture of asphalt concrete mixes in a number of studies [44–46]. However, the values measured do not necessarily agree or directly correlate with those from other methods of determining friction properties [43]. Experimental results indicated that the low-speed friction measurements by the BPT were significantly affected by test surface macrotexture. Hence, the general view that the measured low-speed friction is largely governed by the surface microtexture is not always correct [47]. As mentioned previously, microtexture influences pavement friction at low speeds. Hence, the coefficient of friction at 20 km/h measured by the DFT is considered an indication, not a direct measure, of the pavement microtexture [27,48].

In spite of the absence of standard microtexture characterization methods, there are a number of parameters in the literature proposed for that. These are mostly based on the non-contact measurements discussed in Section 3.1. These include average asperity height (ratio of sum of height of individual asperities to total number of asperities), and average asperity density (ratio of number of

asperity to length of surface considered). The average shape factor (product of the asperity height and density) is also used. Other quantitative estimates of surface microtexture include the previously mentioned roughness – height and volume – parameters [28,33]. Much of these have been reviewed [9]. The LTS (Table 2) also outputs the same parameters used for the macrotexture such as the MPD, ETD, etc within the microtexture wavelength band. Some authors, who employed the equipment for pavement surface microtexture characterization also used variables such as the slope variance and the RMS of the microtexture profile [31].

4. Aggregates and asphalt mixture characteristics

The coefficient of friction is significantly affected by the grading of aggregates used in the production of bituminous mixtures [49]. The extent to which the pavement surface will provide adequate skid resistance depend largely on the aggregate polishing properties [50]. Especially, as the microtexture plays a key role in the development of tire–pavement friction and it is mainly governed by aggregate properties. Asphalt binder may have some measure of influence on microtexture soon after placement. Nevertheless, aggregates make up the bulk of asphalt mixtures and serve as the primary contact medium with vehicle tires [3]. Hence, for adequate frictional performance of the pavement surface, the coarse aggregates for asphalt mixtures must be carefully selected.

4.1. Aggregates properties affecting friction

A number of aggregate properties, which influence pavement frictional performance, alongside test methods for characterizing aggregate frictional properties have been reviewed [3]. Salient points from the aforementioned work are summarized in the following paragraphs, coupled with information from other sources.

4.1.1. Hardness and mineralogy

This largely determines the wear characteristics of the aggregate. Aggregates with hard, strongly bonded, interlocking mineral crystals (coarse grains) embedded in a matrix of soft minerals usually provide the highest levels of long-term friction [3,12]. The hardness of an aggregate is usually determined by the Mohs hardness test. This measures the resistance of a mineral's surface to scratching on a scale of 1–10, the values increasing with hardness. A combination of hardness values ≥ 6 for hard minerals and 3–5 for soft minerals is desired in a coarse aggregate that provides good pavement frictional performance in terms of a balance of wear and polish resistance [51]. Mineralogy is usually investigated by petrographic analysis, which entails microstructural analysis using optical and scanning electron microscopy (SEM). A 50–70% content of hard minerals, an average crystal size of 200 μm and hard grains with angular tips are thought to provide the best frictional resistance [3].

4.1.2. Polish resistance

The polish resistance of an aggregate refers to its ability to retain its microtexture after subjection to grinding and shearing by repeated traffic loadings. It is mainly evaluated by two widely used and accepted tests – the polished stone value (PSV) and acid insoluble residue (AIR) tests. Values of 30–35 for the PSV and 50–70% for the AIR tests are thought to provide good frictional resistance. In addition, there are other polish resistance test methods including the Wehner/Schulze test (W/S) test. The W/S test is reported to be capable of finding the difference in polishing among aggregates in case of similar PSV results [52]. However, suggestions have been made for polishing and testing the mixture, not just the coarse aggregate so as to enable relating the laboratory results to

field frictional performance [53]. Albeit, there is experimental evidence of a strong relationship between mix frictional properties and aggregate PSV and AIR values [54].

4.1.3. Abrasion/wear resistance

This is an indication of the aggregates resistance to mechanical degradation. It is evaluated by the Micro-Deval and Los Angeles (LA) abrasion tests. Percent losses of ≤ 17 –20 in the Micro-Deval test [3] and ≤ 35 –45 in the LA abrasion tests [55] are reported as typical values for good frictional resistance.

4.1.4. Shape, texture and angularity

These characteristics are important for defining micro and macro texture. Sharp and angular coarse aggregate particles interlock and provide greater macrotexture depth. While flat and elongated particles tend to be horizontally oriented resulting in lower macrotexture depth. Hence, the former are preferred to the latter. Two of the most commonly used methods for aggregate shape, texture and angularity are uncompacted void content of coarse aggregate and fractured-faced particles test. Guideline values of $\geq 45\%$ and 90% are recommended for the uncompacted void content and fractured-faced particles, respectively. These are from permanent deformation and rutting concerns, not necessarily for frictional performance [56]. A number of different test methods for aggregate shape, texture and angularity have been identified [57].

Some of the available testing methods for the three parameters are influenced by changes in them during the tests and do not distinguish between changes in two parameters (e.g. texture and angularity). Hence, the Aggregate Imaging System (AIMS), which provides the distribution of each of the parameters in an aggregate sample was recommended for analysis of the parameters. AIMS uses a mechanism for capturing images at different resolutions based on particle size and measures the three dimensions of aggregates [57]. It gives detailed analysis of texture and is able to rapidly and accurately quantify the influence of polishing on texture [58]. However, it was reported in a recent study that macrotexture results from the sand patch test (MTD) did not show a good correlation ($R^2 = 0.009$) with the ETD results from AIMS analysis [45]. Nevertheless, the microtexture results from the BPT (see Section 3.2) showed good correlation ($R^2 = 0.88$) with AIMS results. These observations might be due to differences in types of aggregates and asphalt mixes considered by the different authors.

4.1.5. Soundness

This is the ability of the aggregate to resist degradation caused by climatic/environmental effects such as wetting and drying, freezing and thawing, etc. It is mainly measured using the magnesium sulfate soundness test. This evaluates the maximum weighted average loss percentage of the aggregate after a number of hydration–dehydration cycles. Higher loss percentages are indicative of unsound aggregates. Maximum loss percentages ranging from 10% to 20% are typical of sound aggregates for good frictional performance [3].

4.1.6. General comments

The following are some of the most commonly used aggregates for pavement surface courses: basalt (trap rock), dolerite, granite, greywacke, river gravel, glacial gravel, dolomite, sandstone, quartzite and steel slag. The first four aggregates are reported as the rock types with the largest number of quarries in the UK [9]. Limestone is not included here as it is very susceptible to polishing and hence not used as aggregate in most pavement surfaces courses. Nevertheless, it is used in lower layers of pavement construction [9,59]. Granites, basalts and crushed gravels are reported to have similar microtexture and comparable polish resistance [44]. Sandstone has a uniform and high texture and is able to retain or regen-

erate its microtexture (recovery to its original asperity) with time [60,61]. In contrast, aggregates such as dolomite and dolerite, which include minerals of similar hardness, are more prone to polishing than gabbro (a type of trap rock) and sandstone [61]. It was observed that sandstone possesses the most uniform texture, and higher skid resistance, compared with quartzite and river gravel [60]. Steel slag is an expansive aggregate often added when high frictional properties are required [62].

There is a paucity of literature comparing the aggregate properties discussed above and the resulting skid resistance of pavements produced from them for a wide range of aggregates at the same time. An attempt in this regard considered 5 aggregates, namely, limestone, dolomite, sandstone, gravel and steel slag [63]. It sought to predict field friction values using regression analysis of laboratory PSV data for the aggregates. However, it was inconclusive probably due to the diversity of aggregates. All the same, it showed average PSV of 37 for sandstone, 30.8 for steel slags, 28.5 (24–35 range) for dolomites, 28 for crushed gravels and 26 for limestones (23.2–29.5 range). This confirms observations made earlier on the aggregates. The authors suggested correlating a PSV value of 25 to a friction number smooth of 27.7 and a friction number ribbed of 30.7 for towed friction trailer measurements of field friction – ASTM E274/E274M [64]. The high frictional property of steel slag is corroborated by observations in which it showed higher average friction numbers (45.2) than natural aggregates – crushed gravel (40), crushed stone (40.5) and dolomite (40.2) for a certain mix type in ASTM E274 friction tests [65].

4.2. Frictional properties of asphalt mixtures

Asphalt pavement is a mixture of coarse and fine aggregates and petroleum-based asphalt binder. The factors affecting tire-pavement friction were identified in Section 2. Based on the factors that are controllable through pavement design, some of the main reasons adduced for low skid resistance on asphalt pavements

are (1) aggregate quality, (2) aggregate gradation, (3) mix design method, and (4) use of higher asphalt content than recommended by the mix design method [66].

The quality of aggregates was discussed in the previous section. The aggregate gradation and the finish quality of the surface mix determines the surface macrotexture. This in turn influences pavement surface drainage [3]. Aggregate gradation has a minor influence on microtexture [45]. Having dealt with the reasons relating to aggregate behavior, we now turn to the reasons related to mix design method. There are three main bituminous mix design methods in general use, vis-à-vis, Hveem, Marshall and Superpave methods. The Superpave method is based upon the volumetric analysis common to the Hveem and Marshall methods. It was meant to replace the Hveem and Marshall methods. It is performance-based in contrast to the empirical basis of the Hveem and Marshall methods. Thus, it is capable of predicting the performance of the constructed pavement unlike the other two methods [67]. Details and comparisons of the different mix design methods are provided in a number of studies [68–70]. In spite of their differences, they all seek to determine optimum contents of aggregates and asphalt binder for use in an asphalt pavement mix.

Based on the asphalt binder manufacturing process and temperatures used, there are two types of asphalt mixes, namely hot mix asphalt (HMA) or warm mix asphalt (WMA). HMA is heated and poured at temperatures between 149 °C and 177 °C, while WMA is manufactured and poured between 93 °C and 121 °C. HMA is the conventionally used mix and predates the WMA, which originated from Europe and was first used in the USA around 1990 [71,72]. HMA is further classified into three categories, based mainly on macrotexture due to aggregate gradation. Salient details of these mixes are provided in Table 3.

The main binding agent in HMA is asphalt (or bitumen) – a dark brown to black, highly viscous, hydrocarbon produced from petroleum distillation residue. It serves as a waterproof, thermoplastic, viscoelastic adhesive in the mix. It is graded based on physical

Table 3
Salient details and frictional properties of asphalt mix classifications.

Asphalt Mix type	Texture-based mix category	Description and salient details [3,71,72]	Comments on frictional properties
Hot Mix Asphalt (HMA)	Dense-graded HMA	Well- or continuously-graded mixture of coarse and fine aggregates, mineral filler and 5–6% asphalt binder. Categorized by nominal maximum aggregate size (ranging from 9.5 mm to 19 mm) into fine-graded and coarse-graded. The former contains higher percentage of sand and small stones than the latter. Proper design and placement leads to relatively impermeable mixes. Mixes are suitable for all pavement layers and traffic conditions	Has similar microtexture values to gap- and open-graded mixes. Shows lower macrotexture depths (typically 0.4–0.6 mm for fine-graded and 0.6–1.2 mm for coarse-graded) than gap- and open-graded mixes [3,44]
	Gap-graded HMA or Stone matrix asphalt (SMA)	Aimed at creating stone-on-stone contact within mixture to improve tire grip and rutting (deformation) resistance. Contains more durable aggregates, higher (polymer-modified) asphalt content (6–9%), fillers and fibers. Hence, it is more expensive than others. Provides benefits of wet weather friction and lower tire noise due to its coarser surface texture. It also shows less severe cracking	Shows macrotexture depths typically exceeding 1 mm but higher than those of dense graded mixes [3,44]. Larger coarse aggregate sizes in the mix gives better performance and rut resistance [73]
	Open-graded HMA or Open-graded friction course (OGFC)	Designed to be water permeable. Hence, uses mostly coarse aggregates, small percentage of sand/mineral filler and 3–6% asphalt binder. Must contain >15% air voids. In addition to OGFC, a second type of open-graded HMA is used as permeable base for drainage of the top layer containing dense and gap-graded mixes. Low-speed traffic and excessive dirt can clog pores and reduce performance	Shows similar microtexture values to other mixture types but larger macrotexture (typically of 1.5–3 mm depth). Observed to show higher friction values than gap- and dense-graded mixes [3,44,65]
Warm Mix Asphalt – (WMA)		Manufactured with less fossil fuels and includes binding materials and additives such as wax, emulsions and zeolites for easy pouring (reduced viscosity) and spreading at low temperature. It is environmental-friendly with less dust, smoke and fumes. WMA is cheaper to produce, and can remain workable for longer period, than HMA	Showed no significant difference in early age skid resistance compared to HMA pavements. Has comparable or superior rutting resistance to HMA mixes [74–76]

characteristics using the penetration (pen), viscosity (virgin, AC or aged, AR, sample) and Superpave performance grading (PG) systems. A more detailed description of asphalt is provided elsewhere [72]. The effect of different types and grades of asphalt binder on the frictional properties of asphalt mixtures is beyond the scope of this review. In addition to the main binding material, WMA includes additional binding materials and additives (Table 3). The most well-known WMA additives are Sasobit, Evotherm, Advera synthetic zeolite, Aspha-Min zeolite and WAM-foam [77–79]. Any of the additives can be introduced in one of three primary ways of producing WMA. The three WMA technologies are foaming techniques (using synthetic zeolites or WAM foam), use of organic or wax additives (Sasobit), and use of chemical additives (Evotherm) [79].

Asi [66] evaluated the skid resistance of asphalt pavements using the British Pendulum Number (BPN) for a number of mixes. The variability in the mixes included mix design method (Marshall and Superpave) and asphalt content (optimum and 0.5% and 1% higher). Other variables were HMA mix type (dense and SMA mixes) and aggregate type (limestone and steel slag). The results showed skid numbers in the order, mix with 30% limestone replacement with steel slag (99.6) > Superpave mix (95.7) > SMA mix (92.4) > Marshall dense mixes in the order of increasing asphalt content (87.2, 81.3 and 73.9). The unusually high skid numbers in the study are probably due to the fact that testing was done on non-trafficked laboratory prepared samples. However, the results highlight the importance of aggregate quality over mix design method for good frictional performance. It also showed the superior performance of the SMA over the dense HMA mix type. The superior performance of the SMA over the dense mixes is probably due to its coarser surface texture (Table 3). The Superpave mix design method performed better than the Marshall method for limestone aggregates. However, different studies have also shown that OGFC and SMA mixes show more consistent performance than Superpave mixes [65,80]. It all depends on the quality and type of aggregate used. This is supported by the observation that there was no statistical evidence of texture change with Superpave and Marshall mix design methods. The nominal maximum size of aggregate seemed to be the key factor that changes macrotexture [46].

A range of different mixes, including, open-, gap- and dense-graded mixes at different ages were investigated [44]. The study was aimed at identifying variables related to friction performance of surface asphalt mixes. It employed BPT for macrotexture (MPD) and laser profiler for microtexture. The macrotexture of the different mixes increased, while microtexture decreased, with increasing age. The MPD was in the order, open-graded > gap-graded (SMA) > dense-graded mixes but the mixes had similar microtexture values. It can be deduced from the study that higher air void content and coarser gradations increases, while denser gradation reduces, macrotexture. This corroborated earlier studies that increased aggregate spacing increased macrotexture, which should improve pavement friction at high speeds [81,82]. However, it differs from the position that higher aggregate spacing gives lower friction (BPN) values. Hence, higher friction would be observed with dense-graded mixes. It is thought that the differences between the above findings is due to differences in the aggregates used. In addition to mixture type, aggregate type also has significant effect on friction results [80].

The effects of speed, water film thickness and tire tread pattern on skid resistance of different asphalt pavements have also been investigated. The skid resistance is essentially independent of water film thickness at low speeds (30–50 km/h). However, it decreases with water depth at higher speeds [83] (Fig. 4). This is due to decrease in the tire-pavement contact area by the water on the pavement surface, which leads to reduction in friction

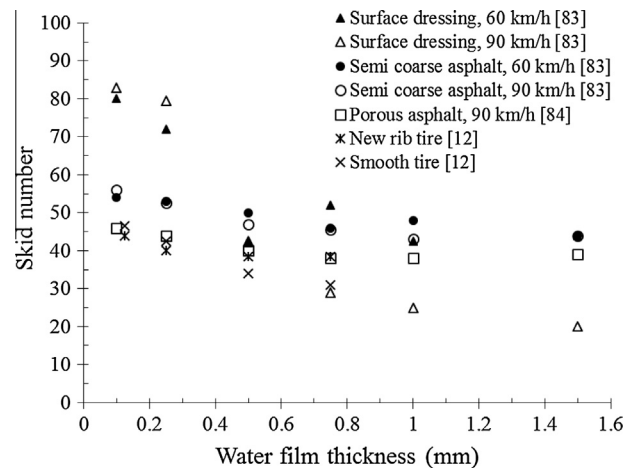


Fig. 4. Effects of water film thickness, speed and tire tread pattern on skid resistance of different asphalt pavements. Note: MPD = 0.48, 1.12 and 2.9 mm for surface dressing, semi coarse asphalt and porous asphalt, respectively. Smooth tire used in related works of Cerezo et al. [83] and Beautru et al. [84]. Measurements made at 64 km/h in Henry [12].

[11]. It has been shown that the speed effect as the water depth increases is negligible for surfaces with higher macrotexture (MPD). Albeit, it becomes significant for surfaces with lower macrotexture [84] (Fig. 4). Smooth tires have historically been shown to be more sensitive to changes in water film thickness than ribbed tires [12] (Fig. 4). Similarly, worn rib tires and half skid tires are more sensitive to the water depth than new rib tires and full skid tires, respectively [12,83].

There is a paucity of literature on the frictional properties of pavements made using WMA. Majority of studies on WMA deal with other performance issues of the mix such as rutting resistance, aging, moisture susceptibility, tensile strength and fatigue and thermal resistance. It has been shown that WMA mixes provides comparable roughness and rutting resistance to HMA mixes [79]. They also have better tensile strength than HMA mixes [74]. In another study, SMA mixes with WMA were reported to show superior performance in moisture susceptibility, rutting resistance and fatigue resistance compared to the same mixes with HMA [76]. It has also been observed that no significant differences existed between the skid resistance of pavements made from WMA and HMA five years after construction [75,85].

5. Influence of environmental factors on skid resistance

This section focusses on the influence of temperature, rainfall and contaminants. These are the major environmental factors that affect tire-pavement friction.

5.1. Influence of temperature

Seasonal variation in skid resistance has been known for over eight decades. The skid resistance of a wet road surface is greater in winter than in summer. Hence, the usual practice of measuring skid resistance during summer, when the lowest values are obtainable, and therefore critical for design. This was rationalized by the position that rubber resilience increases and hysteresis losses become smaller as temperature rises. Both effects combine to reduce the measured value of skid resistance as temperatures increase [86]. The decrease in friction with increasing temperature has also been attributed to changes in the stiffness properties of asphalt and rubber. Changes in the viscosity of water has also been implicated [87]. In light of the above, some studies have developed

equations for strong correlations observed between air and pavement temperatures and friction values [88,89]. In cold climates, winter conditions and maintenance operations tend to increase the microtexture of the aggregate. Hence, skid measurements made on a given pavement during or shortly after winter may be higher than those made during late summer or fall [12]. Evidence from photomicrographs of in-service pavements have shown that surface microroughness increases to a maximum during winter due to natural weathering of aggregates. While much of aggregate microroughness is removed during the summer due to more polishing from traffic [17]. This, and the above position on temperature provides a possible explanation for observed seasonal variation in skid measurements.

5.2. Influence of rainfall

Rainfall also causes a short term variation in skid resistance. Skid measurements made shortly after rainfall may show higher values than those during dry periods. This is linked with the effect of contaminants such as detritus (e.g. dust) and vehicle oil droppings. Water applied in skid tests done during the dry period mixes with the dust, detritus and oil thus reducing friction. This effect is reduced for measurements made shortly after periods of rain [12]. This is because the pavements are less contaminated at such times as rainfall washes away some of the contaminants. It has also been shown that skid numbers decrease and reach a minimum value after 7 days of no rainfall. The lowest value is then maintained until the next significant rainfall after which it increases [90]. Nevertheless, there are disagreements on skid resistance variation arising from pavement surface contamination and rainfall. For instance, it was posited that contamination of the pavement surface could be eliminated as a cause of the observed variation in skid resistance [88]. Thus, it is logical to assert that the mechanisms by which rainfall causes variations in skid resistance are not well understood to permit reliable modeling [13,91]. Moreover, it may not be possible to properly account for the inter-relationship between the effects of temperature and rainfall. Limited observations show that microtexture is affected by temperature, whereas macrotexture is affected by rainfall and freeze-thaw cycles [44].

5.3. Influence of contaminants

The effects of contaminants on pavement surface aggregates has been studied. Addition of contaminants on various aggregates subjected to accelerated polishing resulted in significant behavioral differences. Addition of hard but fine-grained contaminants significantly reduced measured skid resistance as it helped polished the aggregate surface. While addition of coarse but hard contaminants significantly improved measured skid resistance as it helped scratched and abraded the surface [13]. There is need to extend the same investigations to real contaminant types that end up on pavement surfaces and their influence on different types of aggregate. Studies quantifying the rate the skid resistance changes with the period after the last rainfall as a function of aggregate type are required. This would provide an improved understanding of the previously mentioned rainfall-contamination nexus on skid resistance variation.

6. Modeling of tire-pavement friction

Modeling of the interaction between a tire and an asphalt pavement would entail five aspects. These are pavement surface texture and roughness modeling, tire rubber modeling, and tire-pavement

contact modeling. Other aspects are modeling of asphalt mixes, and asphalt pavement surface skid resistance modeling.

6.1. Pavement surface texture and roughness modeling

In Section 3.2, the MPD was mentioned as a parameter for characterizing pavement surface texture. It may be derived from the MTD of the sand patch test or directly based on laser measurements. It is aimed at modeling a fraction of the pavement profile frequency spectrum – the macrotexture. A generalized simple model recently established good correlation between the MTD and MPD [92]. It fits the data of many asphalt wearing courses. However, the MTD-MPD relationship diverges from linearity when open-graded mixtures are considered. Models of surface texture can also utilize measurements of the entire profile spectrum from laser profilometry described in Section 3.2. The spectral analysis approach transforms the longitudinal road profile into the frequency domain [93]. It has been used to highlight the influence of megatexture on noise, vibrations and rolling resistance [30]. Another approach is by idealizing a laser profile as a spectrum. Nevertheless, this leads to loss of information on surface properties relevant to skid resistance modeling [93]. Possible solutions include using indicators such as MPD and MTD, and use of continuous wavelet and Hilbert-Huang transforms [94,95].

The use of fractals in pavement surface texture modeling has also been considered. A fractal can be described as a set of points or a pattern that is apparently similar (repeating pattern) at every scale. Fractal analysis is particularly useful for characterization of profiles that exhibit self-similarity and appear the same under any magnification [9]. Fractal parameters are used to estimate the height variation of a set of surface laser profiles. A surface measure relating to macrotexture and microtexture can then be obtained. This seems to correlate well with measured variation in height and skid resistance numbers [96–98]. Fractal texture models consisting of three different scales (ranges) have also been developed for description of the micro, macro and megatexture [98,99].

Surface texture modeling also includes 3D models of pavement surfaces generated by the CRP technique discussed in Section 3.1. The models have also been deployed in investigation of tire-pavement contact and its effect on wear and asphalt durability [100,101]. A related photometric stereovision technique employed a surface photometric model, based on Lambert's model for body reflection [102], to characterize the photometric behavior of pavement surfaces [103]. Color/relief separation was done from three images taken at three different lighting conditions and from the photometric model of the surface. The image resolution was 0.05 mm, which is within the microtexture range. Links between relief, color and grey-level can then be put in equations. This modeling method permits assessment of surface roughness by means of image-based descriptors. Roughness descriptors also showed correspondence with friction values [103]. Finite element (FE) meshes of the surface texture of asphalt pavements have also been deployed for modeling the effect of micromechanical pavement surface morphology on tire-pavement friction [14]. Asphalt surface morphologies are captured using an X-ray tomographer. Micromechanical FE meshes for different types of asphalt pavements can then be developed from the captured images using proprietary software (e.g. Simpleware).

6.2. Tire rubber modeling

A passenger car tire consists of layers of belts, plies, and bead steel embedded in rubber. Its structural complexity and viscoelastic behavior makes its relationship to skid resistance complex. The application of load to tire rubber causes elastic deformation up to

Table 4
Assumptions/principles and rationale for some major models for asphalt mixtures.

Assumption/principle	Comments	Selected references
Linear visco-elastic behavior	Used spring-dashpot analogs like Burger's model, generalized Maxwell and/or Kelvin models, and Huet-Sayegh model. Response of mixes described using a small number of parameters	[113–117]
Elasto-visco-plastic behavior	The first group focused on aspects of the 3D elasto-visco-plastic response and their implementation in FE software for FE analyses of pavements The second group focused on elasto-visco-plastic response not bound by limitation of incompressibility. Consists of elasto-plastic and visco-elastic components acting in parallel	1st group [118–120] 2nd group [121,122]
Correspondence principle – generation of non-linear visco-elastic models from non-linear elastic models	Used for investigation of various aspects of the inelastic response of asphalt mixes	[109–111,123–125]
Multiplicative decomposition of the total deformation gradient into elastic and inelastic components	Admits that local unstressed intermediate configurations that evolve with the development of inelastic deformations exists	[126–128]

large strain values. However, typical rubber materials show a non-linear elastic stress–strain relationship. Hence, they are termed as viscoelastic materials since their response to loading is a function of strain rate and temperature. The Pacejka “Magic Formula” tire models, a series of empirical tire design models, is widely reported to fit a wide range of tire constructions and operating conditions. The following is the general form of the Magic formula:

$$F(\alpha) = D \sin(C \arctan(B(1 - E)\alpha + E \arctan(B\alpha))) \quad (5)$$

where F is a force or moment resulting from a slip parameter, α while B , C , D and E are curve fitting constants. These can be used to generate equations that show the forces generated for different vertical loads, camber angles and slip angles [104].

Due to its viscoelasticity and structural complexity, majority of modeling efforts for tire rubber entail use of viscoelastic and FE models. Reviews of several viscoelastic and FE tire models can be found elsewhere [93,105]. FE models including all tire components like treads, carcass, piles, etc were recently developed. The tire was tested under static loading conditions to obtain its overall deformation characteristics, especially the tire load-inflation pressure-foot print. The FE simulation results corresponding to the footprint and the deformation were then compared with the measurements of static load deflection tests [14]. However, FE modeling is not yet fast enough for realistic vehicle simulations. Hence empirical models are still necessary [93].

6.3. Tire-pavement contact modeling

The current trend in modeling the tire-pavement contact entails including all the major aspects, i.e. noise, rolling resistance, and skid resistance. A number of different approaches used for modeling tire-pavement contact have been reviewed [93]. Computational contact mechanics models have also been reviewed [14]. Generally, implicit time integration algorithms are often applied for the solution of tire-contact problems together with a fine discretization of tire with huge numbers of finite elements. A combination of implicit and explicit time integration schemes may be employed for the simulation of rolling contact problems on real pavement surfaces. This would include phenomena such as heat generation and conduction, hydroplaning, noise etc [14].

Tire-contact problems can usually be analyzed using steady-state analysis (mixed Lagrangian/Eulerian approach) or transient state analysis (Lagrangian approach). In the former approach, the tire is a fixed set to an observer in the reference frame. While materials flow through the refined stationary mesh. Frictional effects, inertia effects and history effects in the material are accounted for. The mesh can deform due to these effects. In the latter approach, the tires rolls and, turn after turn, the elements touch and leave the contact area to an observer in the reference frame.

The displacements and velocities are calculated in terms of quantities known at the beginning of the increment. No iterations and tangential stiffness matrix are required unlike in steady-state analysis [14]. The FE models developed for surface texture and the calibrated tire model mentioned in Sections 6.1 and 6.2 respectively, were integrated into a thermo-mechanical tire-pavement interaction model. These were used for determination of the temperature development in the tire body and its eventual effect on friction performance [106]. The wet friction performance of different asphalt surface morphologies of open-graded and close-graded mixes were also studied using the developed FE model [14,107].

6.4. Modeling of asphalt mixtures

Asphalt mixtures exhibit elasto-visco-plastic characteristics even at small strains. They are sensitive to strain rate and temperature. Hence, it is difficult to fully model the various stress state encountered by asphalt mixtures during their design life. The major models for asphalt mixtures are based on different assumptions regarding the behavior of the material. Some of these are summarized in Table 4 with comments on the rationale for the assumptions/principles. Selected references, which highlight the assumptions/principles are also included. Much of the information in Table 4 is extracted from Villani [15].

The Huet-Sayegh model with only six parameters is reported to simulate in an excellent way the behavior of asphalt mixes in cycling tests over very wide range of frequencies. However, its main disadvantage is the absence of a viscous element for simulating permanent deformation in contrast with the more familiar Burger's model. Combination of a linear dashpot in series with the Huet-Sayegh model could be used to correct the disadvantage [108]. Some models based on the correspondence principle assumed steady state response and simplified the calculation of pseudo strain [109,110]. Such simplifications are likely to have potential errors in pseudo strain and may be unable to track any permanent pseudo strain that may evolve [111]. Further, it has been shown that models generated by appealing to the correspondence principle do not satisfy the balance of angular momentum principle. However, this constitutes one of the fundamental principles in mechanics that ensures the symmetry of a 3D stress tensor [112]. The admission that local unstressed intermediate configurations that evolve with the development of inelastic deformations exist is thought to be a limiting postulate. Especially, as experimental evidence indicates the development of large volumetric strains with loading for asphalt mixtures [10,15].

It is evident from Table 4 that the thermo-mechanical behavior of asphalt mixtures are mainly simulated using linear elastic and linear visco-elastic models. Nevertheless, these seem insufficient due to the time-, rate-, and temperature-dependence of the

response of asphalt mixtures. This led to development of a 3D microstructure-based computational model that predicts the thermo-mechanical response of asphalt mixtures using a coupled thermo-viscoelastic, thermo-viscoplastic, and thermo-viscodamage constitutive model. The microstructure was reconstructed from slices of 2D X-ray computed tomography images. The model could predict the overall thermo-mechanical response of asphalt mixtures and provide insight on the influence of microstructure on macroscopic response [129]. Further, models based on elasto-visco-plastic behavior do not cover the secondary response and remaining deformations after unloading. Consequently, a recent model was developed to cover the above by combining principles of elasto-visco-plastic response not bound by limitation of incompressibility and multiplicative decomposition [130]. The viscoelastic response of asphalt at any time instant depends on the material's microstructural status, which is in turn a function of the viscoplastic deformation history. Hence, the recent development of a viscoplastic model that captures the material's internal hardening/softening mechanisms. The model is also able to determine the material's macroscopic deformation [131].

6.5. Pavement surface skid resistance modeling

The Penn State model (PSU model) [132], which relates macrotexture to skid resistance, is the most widely used model for tire-pavement skid resistance/friction. It forms the basis of the IFI (Eq. (3)) discussed in Section 2.3. The PSU model describes skid resistance variation with speed and incorporates texture-dependent constants. It can predict pavement surface skid resistance at any slip speed using friction data from the pavement surface at the operating slip speed of the measuring device. The following statistically developed exponential equation expresses the model:

$$SN = SN_0 e^{C_1 V} \quad (6)$$

where SN is the skid resistance (skid number or coefficient of friction), SN_0 is SN at slip speed = 0, V is slip speed, and C_1 is an exponential constant – the product of the reciprocal of SN and the skid number gradient, $\frac{d(SN)}{d(V)}$. C_1 is independent of speed and is related to surface macrotexture [9]. A similar model (the Rado model) complements the PSU model by modeling the maximum friction and maximum speed [133]. These are simple steady state models that are restricted to constant slip speed and constant normal load analysis [25].

The speed is considered in all skid resistance models. However, the applied pressure and rubber temperature are not considered in the development of the aforementioned models. Hence, other models, which considered these parameters, were developed. Such include the Wriggers model, which defines the friction evolution as a function of the normal pressure, the maximum friction coefficient, and the corresponding speed [134]. While another model function of speed and pressure was presented. It is valid only when the temperature variation can be neglected, such as when small

sliding velocities occur (10^{-3} to 10 m/s) [135]. Details of these can be found elsewhere [15].

The drawbacks of the PSU model and its derivative, the IFI, were identified in Section 2.3. Thus, the previously mentioned LuGre model has been suggested. The LuGre model [136,137] is one of a number of friction models that incorporate dynamic effects as done in the Dahl model [138] and the bristles model(s) [139]. Similar to the bristles model(s), the LuGre model treats the frictional interface as a collection of bristles representing surface asperities as shown in Fig. 5. The LuGre model describes 3D tire friction dynamics simplified by assuming constant slip along the contact patch. The model includes the effects of lateral deformation of the tire tread, which leads to varying slip speeds along the contact patch [93]. It employs physically meaningful parameters to represent the main attributes of tire/pavement friction. Eqs. (7)–(9) expresses simplified forms of the LuGre model, especially the average deflection of the bristles and the friction force [140].

$$\dot{Z} = V - \frac{|V|}{G(V)} Z \quad (7)$$

$$G(V) = \frac{1}{\sigma_0} \left(F_C + (F_S - F_C) e^{-(V/V_S)^2} \right) \quad (8)$$

$$F_L(V, Z) = \sigma_0 Z + \sigma_1 \dot{Z} + \sigma_2 V \quad (9)$$

where \dot{Z} is the average deflection of the bristles when there is a relative velocity, V , between the two surfaces. $G(V)$ is a function that allows the model to accommodate a higher static coefficient of friction than dynamic coefficient of friction, with one of its possible forms shown in Eq. (8). Regarding the additional terms in Eq. (8), F_C is the kinetic friction force; F_S is the static friction force; σ_0 is the aggregate bristle stiffness; and V_S is the Stribeck velocity. For the additional terms in Eq. (9), F_L is the LuGre friction force; σ_1 is a damping coefficient and σ_2 accounts for viscous friction.

More recent analytical models express skid resistance as a function of mixture gradation, aggregate texture and traffic level. A model was developed based on comprehensive laboratory and field measurements and analysis of asphalt mixture surface characteristics [141]. The measurements included friction, texture and skid resistance. The multi-step model is able to provide an estimate of the skid number in the field. The steps involved include, estimation of the IFI using CTMeter and DFT field measurements. The IFI is then expressed as a function of the number of polishing cycles in the second step. While in the third and final step, the IFI is expressed as a function of some measure of traffic instead of number of polishing cycles [141]. A similar model for predicting resistance to friction loss incorporates parameters that describe aggregate shape characteristics, aggregate resistance to abrasion and polishing, aggregate gradation, and polishing cycles. It can be used to select the proper aggregate type and aggregate gradation needed to provide adequate asphalt pavement skid resistance [27].

7. Concluding remarks

Key parameters influencing measurements of skid resistance of asphalt pavements have been identified and reviewed. A brief overview of some of the most common approaches to modeling the major aspects of tire-pavement friction has also been provided. This paper has provided an overview of some of the latest references on the above subjects not covered in previous reviews. Inconsistencies in the currently used IFI for harmonization of friction measurements were identified. The LuGre model was then suggested in place of the underlying PSU model. Pavement texture measurements have evolved from 2D to 3D methods with the latter capable of covering micro, macro and megatexture scales. 3D

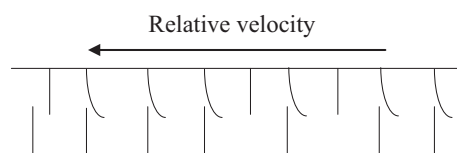


Fig. 5. Analogy between surface asperities and bristles in the LuGre model frictional interface.

measurements also give an indication of the extent of physical changes that cannot be achieved using 2D line profiles.

The frictional performance of asphalt pavements largely depend on the type and quality of coarse aggregates in the asphalt mixture. Aggregates such as trap rock, sandstone and steel slag are noted for their relatively higher frictional performance. The use of Superpave or Marshall mix design methods does not seem to have significant effect on pavement frictional performance. The different HMA classifications generally have similar microtextures. Their frictional performance follows the same order as their macrotextures. There are no significant differences between the skid resistance of pavements made from WMA and HMA up to five years after construction. Further, it is currently not possible to properly account for the inter-relationship between the effects of temperature and rainfall on skid resistance variation.

Modeling efforts on tire-pavement interaction entailing models for surface texture, tire rubber, tire-pavement contact, asphalt mixtures and pavement surface skid resistance were reviewed. There is still a need to develop experimentally-validated models for predicting asphalt pavement skid resistance, especially for warm surfaces. Such models must take into account rheological and geometric characteristics of tires, material and multi-scale surface texture characteristics of pavements and the influence of environmental factors. The existence of models that predict the evolution of skid resistance would help complete data from periodic measurements of pavement surface characteristics. The authors are currently working on developing such models. The following are some other areas where there is need to bridge the information gap.

- (i) Comparisons of aggregate properties and the resulting skid resistance of pavements produced from them for a wide range of aggregates at the same time.
- (ii) Extensive testing on the frictional properties of pavements made using WMA; and
- (iii) Quantification of the influence of aggregate type on the rate the skid resistance changes with the period after the last rainfall.

Acknowledgements

This publication was made possible by an NPRP award (NPRP No. 7-482-2-184: Thermo-Mechanical Tire-Pavement Interaction: Computational Modelling and Field Measurements) from the Qatar National Research Fund (QNRF – a member of The Qatar Foundation). The statements made herein are solely the responsibility of the authors.

References

- [1] Highway Research Board, National Cooperative Highway Research Program Synthesis of Highway Practice 14: Skid Resistance, Highway Research Board, National Academy of Sciences, Washington, D.C., 1972.
- [2] T. Andriejuskas, V. Vorobjovas, V. Mielonas, Evaluation of skid resistance characteristics and measurement methods, in: D. Cygas, T. Tollazzi (Eds.), The 9th International Conference “Environmental Engineering”, VGTU Press, 2014.
- [3] J.W. Hall, K.L. Smith, L. Titus-Glover, L.D. Evans, J.C. Wambold, T.J. Yager, et al., Guide for Pavement Friction Contractor’s Final Report for National Cooperative Highway Research Program (NCHRP) Project 01-43, Transportation Research Board of the National Academies, Washington, D. C., 2009. Available: <http://onlinepubs.trb.org/onlinepubs/nchrp/nchrp_w108.pdf> (Accessed June 2015).
- [4] C.-G. Wallman, H. Åström, Friction Measurement Methods and the Correlation Between Road Friction and Traffic Safety – A Literature Review Report of the Swedish National Road and Traffic Institute, VTI meddelande 911A, Linköping, Sweden, 2001. Available: <<http://www.vti.se/en/publications/pdf/friction-measurement-methods-and-the-correlation-between-road-friction-and-traffic-safety.pdf>> (Accessed June 2015).
- [5] P. Cairney, Skid Resistance and Crashes; A Review of the Literature Research Report ARR 311, ARRB Transport Research, Vermont South, Australia, 1997.
- [6] K. Anupam, S. Srirangam, A. Scarpas, C. Kasbergen, Influence of temperature on tire-pavement friction: analyses, Transp. Res. Rec. J. Transp. Res. Board 2369 (2013) 114–124.
- [7] AASHTO, Guide for Pavement Friction, first ed., American Association of State Highway and Transportation Officials (AASHTO), Washington DC, 2008.
- [8] S.H. Dahir, Review of aggregate selection criteria for improved wear resistance and skid resistance of bituminous surfaces, J. Test. Eval. 7 (5) (1979) 245–253.
- [9] A. Dunford, Friction and the texture of aggregate particles used in the road surface course PhD thesis, University of Nottingham, UK, 2013.
- [10] S.M.J.G. Erkens, Asphalt Concrete Response – Determination, Modeling and Prediction PhD thesis, Delft University of Technology, The Netherlands, 2002.
- [11] G.W. Flintsch, K.K. McGhee, Izeppi E. de León, S. Najafi, The Little Book of Tire Pavement Friction Surface Properties Consortium, 2012. Available from: <https://secure.hosting.vt.edu/www.apps.vti.vt.edu/1-pagers/CSTI_Flintsch/The%20Little%20Book%20of%20Tire%20Pavement%20Friction.pdf> (Accessed October 2015).
- [12] J.J. Henry, Evaluation of Pavement Friction Characteristics. NCHRP Synthesis 291, National Cooperative Highway Research Program (NCHRP), Washington, D.C., 2000.
- [13] D.J. Wilson, The Effect of Rainfall and Contaminants on Road Pavement Skid Resistance New Zealand Transport Agency research report 515, 2013. Available: <<https://www.nzta.govt.nz/assets/resources/research/reports/515/docs/515.pdf>>. Accessed November 2015.
- [14] S.K. Srirangam, Numerical simulation of tire-pavement interaction PhD thesis, Delft University of Technology, The Netherlands, 2015. doi: 10.4233/uuid:ccf73339-112f-4fff-b846-a828a6120a3d.
- [15] M.M. Villani, Friction in asphalt concrete mixes: experimental and computational issues PhD thesis, Delft University of Technology, The Netherlands, 2015. <http://dx.doi.org/10.4233/uuid:2930bb7b-e156-4ac7-b9f2-33ce637938f2>.
- [16] S. Najafi, G.W. Flintsch, A. Medina, Linking roadway crashes and tire-pavement friction: a case study, Int. J. Pavement Eng. (2015), <http://dx.doi.org/10.1080/10298436.2015.1039005> (in press).
- [17] R.H. Smith, Analyzing Friction in the Design of Rubber Products and their Paired Surfaces, CRC Press (Taylor & Francis Group), Boca Raton, FL, 2008.
- [18] R.H. Smith, Measuring rubber friction forces individually, Rubber World 243 (4) (2011) 20–23.
- [19] G. Descornet, B. Schmidt, M. Boulet, M. Gothie, M.-T. Do, J. Fafie, et al., Harmonization of European Routine and Research Measuring Equipment for Skid Resistance HERMES Final Report, 2006, p. 161.
- [20] M.-T. Do, P. Roe, Report on State-of-the-Art of Test Methods TYROSAFE project deliverable D04, 2008, p. 89.
- [21] T.J. Yager, Good pavement texture = good tire friction, in: 4th Safer Roads Conference, Cheltenham, UK, 2014.
- [22] S. Najafi, G.W. Flintsch, K.K. McGhee, Assessment of operational characteristics of continuous friction measuring equipment (CFME), Int. J. Pavement Eng. 14 (8) (2013) 706–714.
- [23] J. Wambold, C. Antle, J. Henry, Z. Rado, International PIARC Experiment to Compare and Harmonize Texture and Skid Resistance Measurement Permanent International Association of Road Congress (PIARC) Report, C-1 PIARC Technical Committee on Surface Characteristics, France, 1995.
- [24] ASTM, E1960-07: Standard Practice for Calculating International Friction Index of a Pavement Surface, American Society for Testing and Materials (ASTM), West Conshohocken, PA, 2011.
- [25] MPN Rajapakshe, Physically meaningful harmonization of tire/pavement friction measurement devices PhD thesis, University of South Florida, 2011. Available: <<http://scholarcommons.usf.edu/etd/3303>>. Accessed December 2015.
- [26] PIARC, Report of the committee on surface characteristics, in: Permanent International Association of Road Congress (PIARC) XVIII World Road Congress, Brussels, 1987.
- [27] E. Kassem, A. Awed, E. Masad, D.N. Little, Development of predictive model for skid loss of asphalt pavements, Transp. Res. Rec. J. Transp. Res. Board 2372 (2013) 83–96.
- [28] G. McQuaid, P. Millar, D. Woodward, S. Friel, Use of close range photogrammetry to assess the micro-texture of asphalt surfacing aggregate, in: International Journal of Pavements Conference, São Paulo, Brazil, Paper 219-2, 2013.
- [29] P.G. Roe, R. Sinhal, The Polished Stone Value of Aggregates and In-Service Skidding Resistance TRL Report 322, TRL, Crowthorne, UK, 1998.
- [30] G. Descornet, Criterion for optimizing surface characteristics, Transp. Res. Rec. 1215 (1989) 173–177.
- [31] S. Li, S. Noureldin, K. Zhu, Y. Jiang, Pavement surface microtexture: Testing, characterization, and frictional interpretation, in: B. Choubane (Ed.), Pavement Performance: Current Trends, Advances, and Challenges; ASTM STP 1555, American Society for Testing and Materials (ASTM), West Conshohocken, PA, 2012, pp. 59–76. doi: 10.1520/STP104426.
- [32] G. Bittelli, A. Simone, F. Girardi, C. Lantieri, Laser scanning on road pavements: a new approach for characterizing surface texture, Sensors 12 (2012) 9110–9128.
- [33] G. McQuaid, P. Millar, D. Woodward, A comparison of techniques to determine surface texture data, in: Civil Engineering Research in Ireland Conference, Belfast, Ireland, 2014.

- [34] P. Vacura, L. Lane, D. Cheng, Caltrans Using Fog and Rejuvenating Seals on State Highways for Preventative Maintenance Newsletter of the California Pavement Preservation Center No. 28, December, 2013, pp. 4–7. Available: <<https://www.csuchico.edu/cp2c/documents/Newsletters/NL28Dec13-web.pdf>>. Accessed December 2015.
- [35] A. Dunford, A.R. Parry, P.H. Shipway, H.E. Viner, Three-dimensional characterisation of surface texture for road stones undergoing simulated traffic wear, *Wear* 292–293 (2012) 188–196.
- [36] P. Millar, Non-contact evaluation of the geometric properties of highway surfacing textures using close range photogrammetry PhD thesis, University of Ulster, UK, 2013.
- [37] D. Woodward, P. Millar, G. McQuaid, Use of 3D modelling techniques to better understand road surface textures, in: 4th International Safer Roads Conference, Cheltenham, UK, 2014.
- [38] G. McQuaid, P. Millar, D. Woodward, Use of 3D modeling to assess pothole growth, in: A.F. Nikolaidis (Ed.), 6th International Conference on Bituminous Mixtures and Pavements, Thessaloniki, Greece, Taylor & Francis Group, London, 2015, pp. 161–166.
- [39] P. Millar, D. Woodward, Noncontact assessment of highway surface vulnerability to water induced damage, *Int. J. Pavements* 10 (1–2–3) (2011) 39–49.
- [40] P. Millar, D. Woodward, A. Woodside, Use of close range terrestrial photogrammetry to assess accelerated wear of asphalt concrete surface course mixes, in: In 6th International Conference on Maintenance and Rehabilitation of Pavements and Technological Control (MAIREPAV6), 2009, pp. 734–740.
- [41] ASTM, E1845: Standard Practice for Calculating Pavement Macrotecture Mean Profile Depth, American Society for Testing and Materials (ASTM), West Conshohocken, PA, 2015.
- [42] W. Wang, X. Yan, H. Huang, X. Chu, M. Abdel-Aty, Design and verification of a laser based device for pavement macrotecture measurement, *Transp. Res. C* 19 (4) (2011) 682–694.
- [43] ASTM, E303-93: Standard Test Method for Measuring Surface Frictional Properties using the British Pendulum Tester, American Society for Testing and Materials (ASTM), West Conshohocken, PA, 2013.
- [44] A. Ongel, Q. Lu, J. Harvey, Frictional properties of asphalt concrete mixes, *Proc. Inst. Civ. Eng. Transp.* 162 (1) (2009) 19–26.
- [45] V.M. Araujo, I.S. Bessa, V.T.C. Branco, Measuring skid resistance of hot mix asphalt using the aggregate image measurement system (AIMS), *Constr. Build. Mater.* 98 (2015) 476–481.
- [46] M. Stroup-Gardiner, J. Studdard, C. Wagner, Evaluation of hot mix asphalt macro- and microtexture, *J. Test. Eval.* 32 (1) (2004) 7–16.
- [47] Y. Liu, T.F. Fwa, Y.S. Choo, Effect of surface macrotecture on skid resistance measurements by the British Pendulum Test, *J. Test. Eval.* 32 (4) (2004) 304–309.
- [48] Z. Wu, B. King, C. Abadie, Z. Zhang, Development of design procedure to predict asphalt pavement skid resistance, *Transp. Res. Rec. J. Transp. Res. Board* 2306 (2012) 161–170.
- [49] X. Zhang, T. Liu, C. Liu, Z. Chen, Research on skid resistance of asphalt pavement based on three-dimensional laser-scanning technology and pressure-sensitive film, *Constr. Build. Mater.* 69 (2014) 49–59.
- [50] G.A. Ali, R. Al-Mahrooqi, M. Al-Mammari, N. Al-Hinai, R. Taha, Measurement, analysis, evaluation, and restoration of skid resistance on streets of Muscat, *Transp. Res. Rec.* 1655 (1998) 200–210.
- [51] S.H. Dahir, J.J. Henry, Alternatives for the Optimization of Aggregate and Pavement Properties Related to Friction and Wear Resistance Report No. FHWA-RD-78-209, Federal Highway Administration (FHWA), Washington, D. C., 1978.
- [52] J. Daskova, J. Kudrna, The experience with Wehner/Schulze procedure in the Czech Republic, in: *SIIV – 5th International Congress – Sustainability of Road Infrastructures*, vol. 53, Procedia-Social and Behavioral Sciences, 2012, pp. 1034–1043.
- [53] NCAT, Coarse aggregate polishing resistance is not enough to ensure adequate surface friction, Asphalt Technology E-News, National Center for Asphalt Technology (NCAT) at Auburn University, Auburn, AL, 2013. Volume 25, No. 1 Available: <<http://www.ncat.us/info-pubs/newsletters/spring-2013/coarse-aggregate-polishing-resistance.html>>. Accessed December 2015.
- [54] E. Masad, A. Rezaei, A. Chowdhury, P. Harris, Predicting Asphalt Mixture Skid Resistance Based on Aggregate Characteristics Report No. FHWA/TX-09/0-5627-1, Federal Highway Administration (FHWA), Washington, D.C., 2009. Available: <<http://d2dtf5nnpf0r.cloudfront.net/tti.tamu.edu/documents/0-5627-1.pdf>>.
- [55] FHWA, Surface Texture for Asphalt and Concrete Pavements. Technical Advisory T 5040.36, U.S. Department of Transportation, Federal Highway Administration, Washington, D.C., 2005. Available: <<https://www.fhwa.dot.gov/pavement/t504036.cfm>>. Accessed December 2015.
- [56] B.D. Prowell, J. Zhang, E.R. Brown, Aggregate Properties and the Performance of Superpave-Designed Hot Mix Asphalt NCHRP Report 539, National Cooperative Highway Research Program (NCHRP), Washington, D.C., 2005. Available: <http://onlinepubs.trb.org/onlinepubs/nchrp/nchrp_rpt_539.pdf>. Accessed November, 2015.
- [57] E. Masad, T. Al-Rousan, J. Button, D. Little, E. Tutumluer, Test Methods for Characterizing Aggregate Shape, Texture, and Angularity NCHRP Report 555, National Cooperative Highway Research Program (NCHRP), Washington, D.C., 2007. Available: <http://onlinepubs.trb.org/onlinepubs/nchrp/nchrp_rpt_555.pdf>. Accessed October 2015.
- [58] A. Luce, E. Mahmoud, E. Masad, A. Chowdhury, Relationship of aggregate microtexture to asphalt pavement skid resistance, *J. Test. Eval.* 35 (6) (2007) 578–588.
- [59] Y. Senga, A. Dony, J. Colin, S. Hamlat, Y. Berthaud, Study of the skid resistance of blends of coarse aggregates with different polish resistances, *Constr. Build. Mater.* 48 (2013) 901–907.
- [60] E.A. Masad, A. Luce, E. Mahmoud, A. Chowdhury, Relationship of Aggregate Texture to Asphalt Pavement Skid Resistance Using Image Analysis of Aggregate Shape Final Report for Highway IDEA Project 114, Transportation Research Board, Washington D.C., 2007. Available: <http://onlinepubs.trb.org/onlinepubs/archive/studies/idea/finalreports/highway/nchrp114final_report.pdf>. Accessed December 2015.
- [61] M. Wasilewska, Analysis of coarse aggregate microtexture in polishing process, in: S.O. Ekelu, M. Dundu, X. Gao (Eds.), Proceedings of the First International Conference on Construction Materials and Structures, IOS Press, Johannesburg, South Africa, 2014, pp. 581–586.
- [62] S.A. Beshears, E. Tutumluer, Reclaimed Asphalt Pavement with Steel Slag Aggregate – Successful Use in Illinois Pavements TR News 288 (September–October), Magazine of the Transportation Research Board, Washington, D.C., Transportation Research Board, Washington, D.C., 2013, pp. 46–47. Available: <<http://onlinepubs.trb.org/onlinepubs/trnews/trnews288rpo.pdf>>. Accessed November 2015.
- [63] T. West, J. Choi, D. Bruner, H. Park, K. Cho, Evaluation of dolomite and related aggregates used in bituminous overlays for Indiana pavements, *Transp. Res. Rec. J. Transp. Res. Board* 1757 (2001) 137–147.
- [64] ASTM, E274/E274M-11: Standard Test Method for Skid Resistance of Paved Surfaces Using a Full-Scale Tire, American Society for Testing and Materials (ASTM), West Conshohocken, PA, 2011.
- [65] S. Li, K. Zhu, S. Noureldin, Evaluation of friction performance of coarse aggregates and hot-mix asphalt pavements, *J. Test. Eval.* 35 (6) (2007) 571–577.
- [66] I.M. Asi, Evaluating skid resistance of different asphalt concrete mixes, *Build. Environ.* 42 (1) (2007) 325–329.
- [67] R.M. Anderson, H.U. Bahia, Evaluation and selection of aggregate gradations for asphalt mixtures using superpave, *Transp. Res. Rec. J. Transp. Res. Board* 1583 (2007) 91–97.
- [68] B.L. Swami, Y.A. Mehta, S. Bose, A comparison of the Marshall and Superpave design procedure for materials sourced in India, *Int. J. Pavement Eng.* 5 (3) (2004) 163–173.
- [69] B. Al-Mistarehi, Superpave system versus Marshall design procedure for asphalt paving mixtures (Comparative study), *Global J. Res. Eng.* 14 (5) (2014) 45–52.
- [70] H. Sadid, R.M. Wabrek, S. Dongare, B. Coryell, A. Ebrahimpour, Materials Acceptance Risk Analysis: Superpave Hot Mix Asphalt Research Report No. FHWA-ID-10-182B, Idaho Transportation Department, Boise, ID, 2010. Available: <<https://itd.idaho.gov/highways/research/archived/reports/Final%20RP182B%20Superpave%20Hot%20Mix%20Asphalt.pdf>>. Accessed December 2015.
- [71] S. Wolf, Understanding the Differences between Hot Mix Asphalt and Warm Mix Asphalt Wolf's Asphalt Paving Blog, 2014. Available: <<http://www.wolfpaving.com/blog/understanding-the-differences-between-hot-mix-asphalt-and-warm-mix-asphalt/>>. Accessed December 2015.
- [72] Pavement Interactive, Mix Types. Article on Pavement Interactive – A site by PaviaSystems, 2010. Available: <<http://www.pavementinteractive.org/article/pavement-typesmix-types/>>. Accessed December 2015.
- [73] G. Sarang, B.M. Lekha, J.S. Geethu, A.U. Ravi Shankar, Laboratory performance of stone matrix asphalt mixtures with two aggregate gradations, *J. Mod. Transp.* 23 (2) (2015) 130–136.
- [74] M. Ameri, S. Hesami, H. Goli, Laboratory evaluation of warm mix asphalt mixtures containing electric arc furnace (EAF) steel slag, *Constr. Build. Mater.* 49 (2013) 611–617.
- [75] S.C. Somé, V. Gaudefroy, D. Delaunay, Effect of vegetable oil additives on binder and mix properties: laboratory and field investigation, *Mater. Struct.* (2015), <http://dx.doi.org/10.1617/s11527-015-0643-1>. in press.
- [76] J. Lee, M.S. Lee, Y. Kim, J. Lim, S. Kwon, S. Hwang, Comprehensive evaluation of warm SMA using wax-based WMA additive in Korea, *J. Test. Eval.* 43 (5) (2014) 1–9.
- [77] G.C. Hurlley, B.D. Prowell, Evaluation of potential processes for use in warm mix asphalt, *J. Assoc. Asphalt Paving Technol.* 75 (2006) 41–90.
- [78] M. Tao, R. Mallick, Effects of warm-mix asphalt additives on workability and mechanical properties of reclaimed asphalt pavement material, *Transp. Res. Rec. J. Transp. Res. Board* 2126 (2009) 151–160.
- [79] J. Zhang, Effects of warm-mix asphalt additives on asphalt mixture characteristics and pavement performance MSc thesis, University of Nebraska, Lincoln, USA, 2010. Available: <<http://digitalcommons.unl.edu/cgi/viewcontent.cgi?article=1011&context=civilengdiss>>. Accessed December 2015.
- [80] Z. Wu, X. Yang, V.L. Das, L.N. Mohammad, Evaluating frictional characteristics of typical wearing course mixtures in Louisiana, *J. Test. Eval.* 41 (4) (2013) 1–11.
- [81] G.C. Page, Open-graded friction courses: Florida's experience, *Transp. Res. Rec.* 1427 (1993) 1–4.
- [82] I.J. Huddleston, H. Zhou, R.G. Hicks, Evaluation of open-graded asphalt concrete mixtures used in Oregon, *Transp. Res. Rec.* 1427 (1993) 5–12.
- [83] V. Cerezo, M.-T. Do, D. Prevost, M. Bouteldja, Friction/water depth relationship–In situ observations and its integration in tire/road friction models, *Proc. Inst. Mech. Eng. J* 228 (11) (2014) 1285–1297.

- [84] V. Beutru, V. Cerozo, M.T. Do, M. Kane, Influence of thin water film on skid resistance, in: SURF 2012 (7th Symposium on Pavement Surface Characteristics), September, France, 2012.
- [85] T.L.J. Wasage, B. Leach, M. Reyes, F. Arain, Performance of foam warm mix asphalt mixes in garrison green calgary, Proc. Ann. Conf. Can. Soc. Civ. Eng. 3 (2013) 2793–2800.
- [86] C.K. Kennedy, A.E. Young, I.C. Butler, Measurement of skidding resistance and surface texture and the use of results in the United Kingdom, in: Surface Characteristics of Roadways, International Research and Technologies: 1st Symposium on Surface Characteristics, State College, Pennsylvania, USA. ASTM STP No. 1031, 1990, pp. 87–102.
- [87] M.A. Khasawneh, R.Y. Liang, Temperature effect on frictional properties of HMA at different polishing stages, Jordan J. Civ. Eng. 6 (1) (2012) 39–53.
- [88] JWH Oliver, Seasonal Variation of Skid Resistance in Australia Special Report No. 37, Australia Road Research Board, Victoria, Australia, 1988.
- [89] S.M. Bazlamit, F. Reza, Changes in asphalt pavement friction components and adjustment of skid number for temperature, J. Transp. Eng. 131 (6) (2005) 470–476.
- [90] B.J. Hill, J.J. Henry, Short-term, weather-related skid resistance variations, Transp. Res. Rec. 836 (1981) 76–81.
- [91] P.D. Cenek, D.J. Alabaster, R. Davies, Seasonal and Weather Normalisation of Skid Resistance Measurements Transfund New Zealand research report 139, 1999.
- [92] F.G. Praticò, R. Vaiana, A study on the relationship between mean texture depth and mean profile depth of asphalt pavements, Constr. Build. Mater. 101 (2015) 72–79. Part 1.
- [93] L.G. Andersen, J.K. Larsen, E.S. Fraser, B. Schmidt, J.C. Dyre, Rolling resistance measurement and model development, J. Transp. Eng. 141 (2) (2015) 04014075.
- [94] F.G. Praticò, Nonstrictly-ergodic signals in road roughness analyses: A theoretical and experimental study, in: Second SIIV International Congress on New Technologies and Modeling Tools for Roads – Application to Design and Management, University of Florence, Italy, 2004.
- [95] Z. Rado, M. Kane, An initial attempt to develop an empirical relation between texture and pavement friction using the HHT approach, Wear 309 (1–2) (2014) 233–246.
- [96] A.G. Kokkalis, G.H. Tsohos, O.K. Panagouli, Consideration of fractals potential in pavement skid resistance evaluation, J. Transp. Eng. 128 (6) (2002) 591–595.
- [97] O.K. Panagouli, A.G. Kokkalis, Skid resistance and fractal structure of pavement surface, Chaos Solitons Fractals 9 (3) (1998) 493–505.
- [98] Z. Rado, Fractal characterization of road surface textures for analysis of friction, in: Proceedings of the Third International Symposium on Pavement Surface Characteristics, Christchurch, New Zealand, 1996, pp. 101–133.
- [99] R.J. Pinnington, A particle-envelope surface model for road–tyre interaction, Int. J. Solids Struct. 49 (3) (2012) 546–555.
- [100] P. Millar, D. Woodward, Close Up and Dirty: A Whistle-Stop Tour of European Highway Surface Textures Asphalt Professional, Issue 42 (January), The Institute of Asphalt Technology, Bathgate, UK, 2010, pp. 14–17.
- [101] P. Millar, D. Woodward, S. Friel, Mapping interfacial stress distributions to digital surface microtopography, in: Third International Surface Friction Conference, Safer Road Surfaces – Saving Lives, Gold Coast, Australia, 2011. Available: <http://uir.ulster.ac.uk/19656/1/Millar_et_al_3rd_Int_Surface_Friction_Conf_Australia_2011.pdf>. Accessed December 2015.
- [102] M. Oren, S.K. Nayar, Generalization of Lambert's reflectance model, in: D. Schweitzer, A. Glassner, M. Keeler (Eds.), Proceedings of the 21st International ACM Conference on Computer Graphics and Interactive Techniques. Association for Computing Machinery (ACM), Orlando, FL, 1994, pp. 239–246 (doi: 10.1145/192161.192213).
- [103] A.B. Slimane, M. Khoudir, J. Brochard, M.T. Do, Characterization of road microtexture by means of image analysis, Wear 264 (5) (2008) 464–468.
- [104] H. Pacejka, Tire and Vehicle Dynamics, third ed., Elsevier, Amsterdam, The Netherlands, 2012.
- [105] M.H.R. Ghoreishy, A state of the art review of the finite element modelling of rolling tyres, Iran. Polym. J. 17 (8) (2008) 571–597.
- [106] S.K. Srirangam, K. Anupam, A. Scarpas, C. Kasbergen, Development of a thermomechanical tyre–pavement interaction model, Int. J. Pavement Eng. 16 (8) (2015) 721–729.
- [107] S. Srirangam, K. Anupam, A. Scarpas, C. Kasbergen, M. Kane, Safety aspects of wet asphalt pavement surfaces through field and numerical modeling investigations, Transp. Res. Rec. J. Transp. Res. Board 2446 (2014) 37–51.
- [108] A.C. Pronk, The Huet–Sayegh model: a simple and excellent rheological model for master curves of asphaltic mixes, in: E. Masad, V.P. Panoskaltis, L. Wang (Eds.), Asphalt Concrete Simulation, Modeling, and Experimental Characterization. R. Lytton Symposium on Mechanics of Flexible Pavements, Baton Rouge, LA, 2006, pp. 73–82. doi: 10.1061/40825(185)8.
- [109] M.E. Kutay, N. Gibson, J. Youtcheff, Conventional and viscoelastic continuum damage (VECD)-based fatigue analysis of polymer modified asphalt pavements (with discussion), J. Assoc. Asphalt Paving Technol. 77 (2008) 395–433.
- [110] D.W. Christensen, R. Bonaquist, Practical application of continuum damage theory to fatigue phenomena in asphalt concrete mixtures (with discussion and closure), J. Assoc. Asphalt Paving Technol. 74 (2005) 963–1002.
- [111] B.S. Underwood, Y.R. Kim, M.N. Guddati, Improved calculation method of damage parameter in viscoelastic continuum damage model, Int. J. Pavement Eng. 11 (6) (2010) 459–476.
- [112] K.R. Rajagopal, A.R. Srinivasa, On the nature of constraints for continua undergoing dissipative processes, Proc. R. Soc. London A 461 (2061) (2005) 2785–2795.
- [113] R. Lytton, J. Uzan, E.G. Fernando, R. Roque, D. Hiltunen, S.M. Stoffels, Development and Validation of Performance Prediction Models and Specifications for Asphalt Binders and Paving Mixes Report No. SHRP-A-357, Strategic Highway Research Program, National Research Council, Washington, DC, 1993. Available: <<http://onlinepubs.trb.org/onlinepubs/shrp/SHRP-A-357.pdf>>. Accessed December 2015.
- [114] R.N. Nilsson, P.C. Hopman, U. Isacson, Influence of different rheological models on predicted pavement responses in flexible pavements, Road Mater. Pavement Des. 3 (2) (2002) 117–149.
- [115] M. Oeser, T. Pellinen, T. Scarpas, C. Kasbergen, Studies on creep and recovery of rheological bodies based upon conventional and fractional formulations and their application on asphalt mixture, Int. J. Pavement Eng. 9 (5) (2008) 373–386.
- [116] F. Olard, H. Di Benedetto, General, “2S2P1D” model and relation between the linear viscoelastic behaviours of bituminous binders and mixes, Road Mater. Pavement Des. 4 (2) (2003) 185–224.
- [117] Q. Xu, M. Solaimanian, Modelling linear viscoelastic properties of asphalt concrete by the Huet–Sayegh model, Int. J. Pavement Eng. 10 (6) (2009) 401–422.
- [118] A. Collop, A. Scarpas, C. Kasbergen, A. de Bondt, Development and finite element implementation of stress-dependent elastoviscoplastic constitutive model with damage for asphalt, Transp. Res. Rec. J. Transp. Res. Board 1832 (2003) 96–104.
- [119] S.M.J.G. Erkens, X. Liu, A. Scarpas, 3D finite element model for asphalt concrete response simulation, Int. J. Geomech. 2 (3) (2002) 305–330.
- [120] E. Levenberg, J. Uzan, Triaxial small-strain viscoelastic-viscoplastic modeling of asphalt aggregate mixes, Mech. Time-Depend. Mater. 8 (4) (2004) 365–384.
- [121] A. Scarpas, A Mechanics Based Computational Platform for Pavement Engineering, TU Delft publication, Delft University of Technology, The Netherlands, 2005. Available: <<http://repository.tudelft.nl/view/ir/uuid%3Aa95d1457-a1a5-4d10-bcbc-7b734c707d44/>>. Accessed December 2015.
- [122] N. Kringos, A. Scarpas, C. Kasbergen, Three dimensional elasto-visco-plastic finite element model for combined physical-mechanical moisture induced damage in asphaltic mixes (with discussion), J. Assoc. Asphalt Paving Technol. 76 (2007) 495–524.
- [123] Y.R. Kim, D.N. Little, One-dimensional constitutive modeling of asphalt concrete, J. Eng. Mech. 116 (4) (1990) 751–772.
- [124] S.W. Park, Y.R. Kim, R.A. Schapery, A viscoelastic continuum damage model and its application to uniaxial behavior of asphalt concrete, Mech. Mater. 24 (4) (1996) 241–255.
- [125] R.A. Schapery, Correspondence principles and a generalized J integral for large deformation and fracture analysis of viscoelastic media, Int. J. Fract. 25 (3) (1984) 195–223.
- [126] J. Murali Krishnan, K.R. Rajagopal, Thermodynamic framework for the constitutive modeling of asphalt concrete: theory and applications, J. Mater. Civ. Eng. 16 (2) (2004) 155–166.
- [127] J. Murali Krishnan, K.R. Rajagopal, On the mechanical behavior of asphalt, Mech. Mater. 37 (11) (2005) 1085–1100.
- [128] E.H. Lee, Elastic-plastic deformation at finite strains, J. Appl. Mech. 36 (1) (1969) 1–6.
- [129] T. You, R.K.A. Al-Rub, M.K. Darabi, E.A. Masad, D.N. Little, Three-dimensional microstructural modeling of asphalt concrete using a unified viscoelastic-viscoplastic-viscodamage model, Constr. Build. Mater. 28 (1) (2012) 531–548.
- [130] M.M. Villani, C. Kasbergen, A. Scarpas, Presti D. Lo, Mechanistic procedure for parameter determination of multiplicative decomposition based constitutive models, Int. J. Pavement Eng. (2015), <http://dx.doi.org/10.1080/10298436.2015.1088154>. in press.
- [131] W. Cao, Y.R. Kim, A viscoplastic model for the confined permanent deformation of asphalt concrete in compression, Mech. Mater. 92 (2016) 235–247.
- [132] M.C. Leu, J.J. Henry, Prediction of skid resistance as a function of speed from pavement texture measurements, Transp. Res. Rec. 666 (1978) 7–13.
- [133] Z. Radó, A study of road surface texture and its relationship to friction PhD thesis, Pennsylvania State University, USA, 1994.
- [134] P. Wriggers, Computational contact mechanics, UK2002.
- [135] U. Nackenhorst, The ALE-formulation of bodies in rolling contact: theoretical foundations and finite element approach, Comput. Methods Appl. Mech. Eng. 193 (39–41) (2004) 4299–4322.
- [136] C. Canudas de Wit, H. Olsson, K.J. Astrom, P. Lischinsky, A new model for control of systems with friction, IEEE Trans. Autom. Control 40 (3) (1995) 419–425.
- [137] J. Deur, V. Ivanović, M. Troulis, C. Miano, D. Hrovat, J. Asgari, Extensions of the LuGre tyre friction model related to variable slip speed along the contact patch length, Veh. Syst. Dyn. 43 (Sup. 1) (2005) 508–524.
- [138] P.R. Dahl, A Solid Friction Model Report No. TOR-0158(3107-18)-1, The Aerospace Corporation, El Segundo, California, 1968. Available: <<http://www.dtic.mil/dtic/tr/fulltext/u2/a041920.pdf>>. Accessed December 2015.
- [139] D.A. Haessig, B. Friedland, On the modeling and simulation of friction, ASME J. Dyn. Syst. Meas. Control 113 (3) (1991) 354–362.
- [140] N.B. Do, A.A. Ferri, O.A. Bauchau, Efficient simulation of a dynamic system with LuGre friction, J. Comput. Nonlinear Dyn. 2 (4) (2007) 281–289.
- [141] A. Rezaei, E. Masad, Experimental-based model for predicting the skid resistance of asphalt pavements, Int. J. Pavement Eng. 14 (1) (2013) 24–35.